Article

Antioxidant, Antimicrobial, and Anti-Inflammatory Effects of *Liriodendron chinense* Leaves

Ya-Li Wang,[||] Qian Ni,[||] Wen-Hao Zeng, Hui Feng, Wei-Feng Cai, Qi-Cong Chen, Song-Xia Lin, Cui-Ping Jiang,* Yan-Kui Yi, Qun Shen,* and Chun-Yan Shen*

Read Online

| ACCESS | Metrics & More | Article Recommendations | Supporting Information |

ABSTRACT: *Liriodendron chinense* has been widely utilized in traditional Chinese medicine to treat dispelling wind and dampness and used for alleviating cough and diminishing inflammation. However, the antioxidant, antimicrobial, and anti-inflammatory effects of *L. chinense* leaves and the key active constituents remained elusive. So, we conducted some experiments to support the application of *L. chinense* in traditional Chinese medicine by investigating the antioxidant, antibacterial, and anti-inflammatory abilities, and to identify the potential key constituents responsible for the activities. The ethanol extract of *L. chinense* leaves (LCLE) was isolated and extracted, and assays measuring ferric reducing antioxidant power, total reducing power, DPPH$^\bullet$, ABTS$^{\bullet+}$, and $^\bullet$OH were used to assess its *in vitro* antioxidant capacities. Antimicrobial activities of LCLE were investigated by minimal inhibitory levels, minimum antibacterial concentrations, disc diffusion test, and scanning electron microscope examination. Further, *in vivo* experiments including macro indicators examination, histopathological examination, and biochemical parameters measurement were conducted to investigate the effects of LCLE on lipopolysaccharide (LPS)-induced acute lung injury (ALI) in mice. LCLE was further isolated and purified through column chromatography, and LPS-induced RAW264.7 cells were constructed to assess the diminished inflammation potential of the identified chemical composites. ABTS$^{\bullet+}$ and $^\bullet$OH radicals were extensively neutralized by the LCLE treatment. LCLE administration also presented broad-spectrum antimicrobial properties, especially against *Staphylococcus epidermidis* by disrupting cell walls. LPS-induced ALI in mice was significantly ameliorated by LCLE intervention, as evidenced by the histological changes in the lung and liver tissues as well as the reductions of nitric oxide (NO), TNF-α, and IL-6 production. Furthermore, three novel compounds including fragransin B2, liriodendritol, and rhamnocitrin were isolated, purified, and identified from LCLE. These three compounds exhibited differential regulation on NO accumulation and IL-10, IL-1β, IL-6, TNF-α, COX-2, and iNOS mRNA expression in RAW264.7 cells induced by LPS. Fragransin B2 was more effective in inhibiting TNF-α mRNA expression, while rhamnocitrin was more powerful in inhibiting IL-6 mRNA expression. LCLE had significant antioxidant, antimicrobial, and anti-inflammatory effects. Fragransin B2, liriodendritol, and rhamnocitrin were probably key active constituents of LCLE, which might act synergistically to treat inflammatory-related disorders. This study provided a valuable view of the healing potential of *L. chinense* leaves in curing inflammatory diseases.
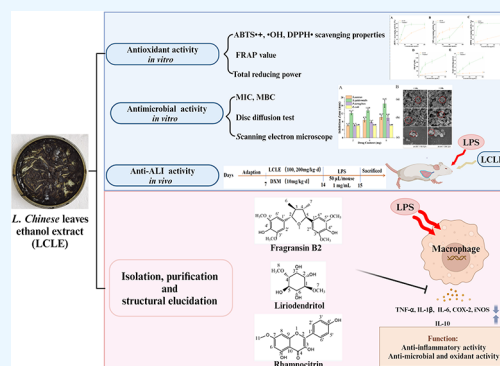
1. INTRODUCTION

Inflammation implies an intensified physiological response to diverse stimuli, and unbridled inflammation has unequivocally been directly associated with a number of diseases, including acute lung injury, sepsis, and cancer.[1] Acute lung injury (ALI) represents a profoundly incapacitating and frequently lethal acute inflammatory disorder, posing a substantial challenge in the field of intensive care medicine.[2] Extensive documentation exists regarding lipopolysaccharide (LPS) that is produced by Gram-negative bacteria, establishing it as a crucial trigger of the inflammatory cascade culminating in the development of ALI.[3] Macrophages are among the principal inflammatory cells, exerting critical functions in preserving homeostasis and regulating various physiological processes. Prior research has established the crucial significance of macrophage development

in LPS-induced ALI, given that macrophages manifest sensitivity to inflammatory stimuli and play a pivotal role in the release of pro-inflammatory cytokines.[4] More precisely, inducible nitric oxide synthase (iNOS) is expressed by macrophages in response to cytokine or microbial stimulation. INOS can promote nitric oxide (NO) generated from L-arginine. NO not only serves as an immune system mediator but also plays roles in regulating blood pressure and

transmissing brain signal.[5,6] Numerous macrophages residing in the pulmonary parenchyma can be promptly, either directly or indirectly, triggered by external stimuli originating within the lung, thereby expediting the advancement of the inflammatory response.[7] As such, macrophages find widespread utility in the initial screening of natural compounds or therapeutic agents aimed at mitigating extremely inflammatory reactions.

The clinical management of ALI includes inhaled vasodilators, mechanical ventilation, and anti-inflammatory medications, including corticosteroids. Dexamethasone (DXM), a glucocorticoid, can alleviate oxidative stress and inflammation in cases of ALI.[8] However, many side effects, including myopathy, altered glucose metabolism, gastrointestinal issues, irritability, mental health disorders, anxiety, insomnia, and an elevated risk of pneumonia, have been linked to DXM.[9] Consequently, it is imperative to develop a safer medication for the treatment of ALI. There exist two clearly delineated species in the *Liriodendron* genus, which is a constituent of the Magnoliaceae family: *Liriodendron tulipifera* L., originating from North America, and *Liriodendron chinense*, deriving from East Asia.[10] Acknowledged as a medicinal herb, *L. chinense* has been recorded in the Compilation of Countrywide Herbal Medicine of China. Traditionally, it is recognized for its therapeutic functions in dispelling wind and dampness, dispersing cold, relieving coughs, and reducing inflammation.[11] An expanding body of research has underscored *Liriodendron's* efficacy in mitigating hyperuricemic nephropathy associated with inflammation and renal fibrosis, its proficiency in mitigating lipid oxidation, and its antimicrobial attributes.[12,13] Nevertheless, the bulk of these studies have gravitated toward investigating *L. tulipifera* L. and *L. chinense* bark, with comparatively fewer inquiries directed toward the *L. chinense* leaves.[14] As such, there is a lack of pharmacological data on the chemical constituents of *L. chinense* leaves. The purpose of this study was to compare and methodically examine the inhibitory impact of chemicals from *L. chinense* leaves in the context of inflammation.

In the current investigation, we validated the efficacy of the ethanol extract of *L. chinense* leaves (LCLE) against oxidative stress, microbial activity, and the attenuation of LPS-induced ALI. Three constituents were isolated and structurally identified, with fragransin B2 and rhamnocitrin found to be previously unreported in LCLE. Subsequently, we subjected them to activity tracing to confirm their efficacy in mitigating LPS-induced inflammation within RAW264.7 cells. The findings showed that rhamnocitrin, liriodendritol, and fragransin B2 had larger inhibitory impacts on NO production than the positive medication dexamethasone, with rhamnocitrin being the most effective. Notably, they targeted different pathways. Fragransin B2 performed superior in inhibiting tumor necrosis factor-α mRNA (TNF-α) expression, while rhamnocitrin was more powerful in inhibiting interleukin-6 mRNA expression. Given that fragransin B2, liriodendritol, and rhamnocitrin were the primary components of LCLE, it is plausible that they are major contributors to its efficacy. These findings significantly advance our knowledge of the bioactive components of *L. chinense* leaves, underscoring the therapeutic potential of fragransin B2, liriodendritol, and rhamnocitrin in inflammatory diseases.

2. MATERIALS AND METHODS

2.1. Chemicals and Solvents. 2,2′-Biazo-bis-3-ethyl-benzothiazoline-6-sulfonic acid (ABTS) and 1,1-diphenyl-2-picrylhydrazyl (DPPH) were accessed from Sigma-Aldrich (St. Louis, MO). LPS and 3-(4,5-dimethyl-2-thiazolyl)-2,5-diphen-yl-2*H*-tetrazolium bromide (MTT) were purchased from Sigma-Aldrich (Shanghai, China). NO content Griess reagent was from Beyotime Biology Science and Technology Co., Ltd., Shanghai, China. Enzyme-linked immunosorbent test (ELISA) kits for detecting interleukin-6 (IL-6) and TNF-α were supplied by NeoBioscience Technology Co., Ltd. (Shenzhen, China). All of the chemicals and reagents used in this study had analytical grades and were available for purchase.

2.2. Plant Material. *L. chinense* leaves were collected from Zhejiang Province, China, in March 2022, and authenticated by the corresponding authors. The substances were dried by putting in an oven for 24 h at 60 °C, shredded in a pulverizer, and stored hermetically.

2.3. Preparation of Ethanol Extract from *L. chinense* Leaves. The powder of *L. chinense* leaves was extracted with 60% ethanol for 3 h with a solid/liquid ratio of 1:10 (v/v). Three repetitions of the preceding steps were made, and then the extracts from each were combined and centrifuged. The supernatant was then gathered, concentrated, dehydrated, and preserved for future research.

2.4. *In Vitro* Antioxidant Activity. *2.4.1. ABTS Radical Scavenging Assay.* Using 96-well microtitration spectrophotometry, ABTS radicals were determined.[15] 7 mM ABTS was added in 95% ethanol. Then the same quantity of 4.9 mM potassium persulfate solution with the prepared 7 mM ABST aqueous solution was put in the shake bed overnight, after which the ABTS radical cation solution's concentration was decreased to 0.26 mM with anhydrous ethanol. Twenty microliter of LCLE with concentrations of 50, 100, 200, 400, 600, and 800 μg/mL, respectively, was added to 180 μL of 0.26 mM ABTS radical cation solution, mixed, and the absorbance was determined at 734 nm after 30 min at 30 °C of incubation. The positive control used as a part of the experiment was vitamin C. The ABTS$^{\bullet+}$ scavenging rate was computed through Formula 1

$$\text{ABTS}^{\bullet+} \text{ scavenging capability (\%)}$$
$$= [\text{OD}_B - \text{OD}_S/\text{OD}_B] \times 100\% \tag{1}$$

where OD_B represents the measurement of anhydrous ethanol and OD_S is the measurement of tested samples.

2.4.2. $^{\bullet}$OH Radical Scavenging Assay. $^{\bullet}$OH radical scavenging activity was assessed using the method previously described.[16] LCLE was diluted with anhydrous ethanol into 50, 100, 200, 400, 600, and 800 μg/mL. Different concentrations of LCLE were then mixed with 50 μL of 60 mM H_2O_2, 50 μL of 9 mM $FeSO_4$, and 50 μL of 9 mM salicylic acid−ethanol. Then, the absorbance of the mixed solutions was measured at 510 nm after 30 min at 37 °C of incubation. The positive control used as a part of the experiment was vitamin C. The $^{\bullet}$OH scavenging rate was computed through Formula 2

$$^{\bullet}\text{OH radical scavenging activity (\%)}$$
$$= [\text{OD}_B - \text{OD}_S/\text{OD}_B] \times 100\% \tag{2}$$

where OD_B represents the measurement of anhydrous ethanol and OD_S is the measurement of tested samples.

2.4.3. DPPH• Radical Scavenging Assay. DPPH• radicals were assessed by utilizing 96-well microtitration spectrophotometry.[17] LCLE was diluted with anhydrous ethanol into solutions with concentrations of 50, 100, 200, 400, 600, and 800 μg/mL. Afterward, 180 μL of 150 μM DPPH• solution was added with different concentrations of LCLE. The reaction mixture was then shaken rapidly for 30 s and incubated in the dark at room temperature for 30 min. Absorbance was measured at 517 nm. In this assay, the solution color changed with the antioxidant reaction of the stable free radical 2,2-diphenyl-1-picrylhydrazyl and produced 2,2-diphenyl-1-picryl-hydrazine. Vitamin C, at concentrations equivalent to LCLE, served as the reference. The DPPH• scavenging rate was computed through Formula 3

DPPH• radical scavenging activity (%)

$$= [OD_B - OD_S/OD_B] \times 100\% \qquad (3)$$

where OD_B represents the measurement of anhydrous ethanol and OD_S is the measurement of tested samples.

2.4.4. FRAP Value Assay. The ferric reducing antioxidant power (FRAP) values of LCLE were measured according to the prior report with a few modest modifications.[18] Initially, the FRAP reagent contains 2.5 mL of $FeCl_3 \cdot 6H_2O$ (40 mM), 2.5 mL of HCl (20 mM), and 25 mL of acetate buffer (0.3 M, pH 3.6). LCLE was diluted with anhydrous ethanol into a series of concentrations of 50, 100, 200, 400, 600, and 800 μg/mL, further mixed with the FRAP reagent. After 30 min of incubation in the dark at room temperature, the absorbance was measured at 595 nm. The FRAP values were calculated according to the relativity between antioxidant capacity and absorbance, and the absorbance was positively correlated with the concentration of Fe(II) solution (1 mM).

2.4.5. Reducing Power Assay. Reducing power assay was employed based on the earlier report with a few minor adjustments.[19] 0.4 mL of LCLE and vitamin C (50, 100, 200, 400, 600, and 800 μg/mL) were combined with 1 mL of $[K_3Fe(CN)_6]$ solution and 0.2 M phosphate buffer (pH 6.6). The solution was mixed and reacted at 50 °C for 20 min. In the end of the reaction, the mixture was quickly cooled in an ice bath and 1 mL of trichloroacetic acid (10%, w/v) solution was added to terminate. 1 mL of distilled water and 0.2 mL of 0.1% ferric chloride solution were mixed with the supernatant of the reaction solution for 10 min. Finally, the absorbance was measured at 700 nm after adequately shaking.

2.5. Antibacterial Activity. *2.5.1. Microbial Strains.* Microbial strains including *Staphylococcus aureus* (ATCC 6538, GDMCC 1. 1220 *S. aureus*), *Escherichia coli* (ATCC 8739, GDMCC 1. 176 *E. coli*), *Pseudomonas aeruginosa* (ATCC 9027, GDMCC 1.443 *P. aeruginosa*), and *Staphylococcus epidermidis* (ATCC 12228, GDMCC 1. 143 *S. epidermidis*) all bought from the Guangdong Culture Collection Center.

2.5.2. Determination of Minimum Inhibitory Concentrations (MIC). The MIC values of LCLE were determined according to da Silva et al. with a few minor modifications.[20] In brief, normal saline was used to dissolve and dilute LCLE samples, together with the conventional antibacterial agent chloramphenicol. Each embraced standard solutions (10^6 CFU/mL) of each of the microorganisms, with varying final concentrations of either the common antimicrobial antibiotic chloramphenicol (1000−15.625 μg/mL) or LCLE (50−1.5625 mg/mL). The positive control, negative control, and medium control were blank bacterial solution, blank LCLE

solution, and medium solution, respectively. The cultivating dishes were kept in an oven at 37 °C for 24 h. Every test was run at least 3 times. MIC was identified as the smallest level with no discernible bacterial growth in the wells.

2.5.3. Determination of Minimum Bactericidal Concentrations (MBC). A 100 μL portion of the subculture solution was collected from each well without any visible bacterial growth, poured onto the medium plate, and incubated for 24 h at the desired temperature. The lowest concentration, MBC, was found to have no newly apparent microbial colonies.

2.5.4. Disc Diffusion Test. This assay was carried out according to the earlier study with slight modifications.[21] 100 μL suspension of bacterium (10^8 CFU/mL) was cultivated on the nutrient agar media. A filter paper (6 mm) was placed in the middle of each dried inoculum with 20 μL of LCLE solution at 200, 100, and 50 mg/mL, respectively. A filter paper with sterile water served as a blank control. Afterward, the inhibition zone diameters (mm) of the pure and LCLE were calculated and compared after 24 h at 37 °C of incubation. Every test was performed in a minimum of three duplicate assays and repeated 3 times.

2.5.5. Scanning Electron Microscope (SEM). The impact of LCLE on cells' microbial appearance was investigated according to SEM observation.[22] LCLE at levels of 1 × MIC and 2 × MIC and sterile normal saline were used to treat the *S. epidermidis* suspensions (10^5 CFU/mL) for 24 h, respectively. Sterile regular saline was considered as the blank control. After the bacteria were fixed in 2.5% glutaraldehyde, excess glutaraldehyde was removed by washing twice with PBS (pH 7.4). Then, fixed bacteria were dehydrated by ethanol at 30, 50, 70, 85, and 90% for once respectively, except 100% for twice, and 15 min each time. Finally, after adding isopentyl acetate, the crucial point was allowed to dry for 8 h. The result was observed in S-3000N SEM (HITACHI Ltd., Japan).

2.6. Animal Treatment and Experimental Design. Thirty-five Kunming mice (male, 6−8 weeks old) were acquired from Southern Medical University Experimental Animal Science and Technology Development Co., Ltd., Guangzhou, China. The Animal Ethics Committee established by Southern Medical University (Guangzhou, China, L2021084) authorized standard procedures for all animal treatments. The animals were kept in a condition of 25 ± 2 °C and 65 ± 5% humidity with 12 h dark/light cycles and had the freedom to obtain food and water.

After acclimatization for 1 week, the animals were randomly divided into five groups according to body weight: the control (CON) group, LPS group, LPS + DXM group (10 mg/kg·day), low-dose LCLE (LPS + L-LCLE) group (100 mg/kg·day), and high-dose LCLE (LPS + H-LCLE) group (200 mg/kg·day), with eight mice in each group. All drugs were suspended in distilled water. The CON group and the LPS group were treated with distilled water by gavage for 7 days. After the last intervention, all groups except the CON group were treated with LPS (50 μL/mouse, 1 mg/mL) by nasal drip for 8 h to induce ALI. Then the mice were sacrificed via cervical dislocation after anesthesia by ethyl ether inhalation to collect the blood and tissue samples (lung and liver) for subsequent detection. The middle lobe of the right lung was weighed in wet weight and dried in an oven at 80 °C for 48 h. The dry weight was determined, and the degree of edema of the lung tissues was assessed by wet weight/dry weight.

2.7. Macro Indicators Examination. The weight of mice in each group was recorded every week during the period of
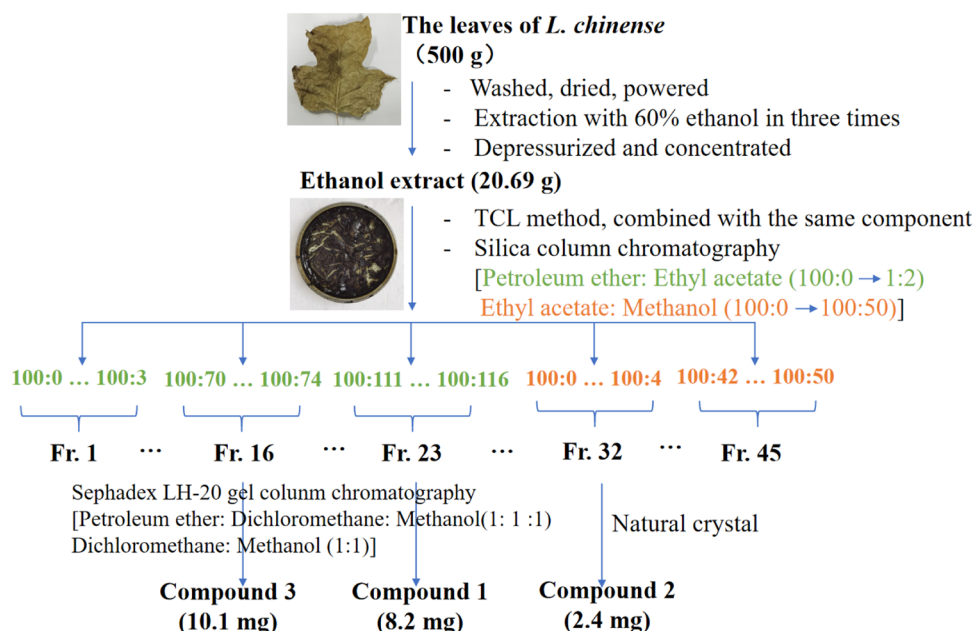
Figure 1. Extraction and isolation procedures of compounds from LCLE.

administration. The wet lungs and livers were weighed to determine organ weight index. The organ wet weight units were expressed as g, and the organ weight index was expressed as % of weight.

2.8. Histopathological Examination. After being cleaned with cold normal saline, the liver and lungs were embedded in paraffin, dehydrated, waxed, and fixed in 4% paraformaldehyde. Then, the livers and lungs were sliced into 4 μm slices. Afterward, hematoxylin and eosin (HE) was used to stain the slices following the commercial instruction. Finally, the pathological alterations in the liver and lung tissues were observed using light microscopy (DM2500, Leica, Wetzlar, Germany).

2.9. Biochemical Parameters Measurement. The lung tissues' biochemical parameters, such as NO, IL-6, and TNF-α, were identified. Briefly, the tissues were divided into tiny pieces and soaked in 0.01 M phosphate buffer at a ratio of 1:9 (g/mL). Griess Reagent (Beyotime Biotechnology Co., Ltd., Shanghai, China) was used to assess the NO content in accordance with the manufacturer's instructions. IL-6 as well as the TNF-α level was measured based on the ELISA kits (NeoBioscience Technology Co., Ltd., Shenzhen, China).

2.10. Extraction, Isolation, and Purification. The procedures of extraction and separation are shown in Figure 1. *L. chinense* leaves (500 g) were extracted 3 times with 60% ethanol by reflux. The crude 60% ethanol extract (20.69 g) of *L. chinense* leaves was then loaded on a column with silica gel (200−300 mesh, 400 g) and eluted with a gradient of petroleum ether-ethyl acetate (100:0−100:200, v/v) and ethyl acetate-methanol (100:0−100:50, v/v). At least 3 column volumes of each gradient were collected. As a result, 45 fractions (Fr.1−Fr.45) were obtained after being combined based on the thin-layer chromatography. Compound 2 (2.4 mg) was obtained as a natural crystal from Fr.32. Fr.23 and Fr.16 were put into a Sephadex LH-20 gel column and dissolved with petroleum ether−dichloromethane−methanol (1:1:1) and dichloromethane−methanol (1:1), thus resulting in compound 1 (8.2 mg) and compound 3 (10.1 mg), respectively.

2.11. NMR Analysis. The chemical compositions of the purified chemicals were clarified by ^{1}H, ^{13}C, and DEPT-135 analyses in CDCl$_3$, D$_2$O, or CD$_3$OD on a Bruker Avance DRX III-600 using standard Bruker pulse sequences.

2.12. High-Performance Liquid Chromatography (HPLC) Analysis. LCLE and chemicals were further confirmed via HPLC analysis using an HPLC instrument (SHIMADZU, Japan, LC-16) equipped with a C18 analytical column (SHIMADZU, Japan), operating at 25 °C, 20 μL of injection volume, and a flow rate of 1 mL/min. The mobile phase for HPLC comprised acetonitrile (eluent A) and 0.2% aqueous phosphoric acid (eluent B). The gradient procedure was as follows: 0−12 min, 20−24% of eluent A; 12−40 min, 24−70% of eluent A. A ultraviolet−visible (UV−vis) detector was used at a wavelength of 190−600 nm.

2.13. Cytotoxicity Assay. According to earlier research, RAW264.7 cells were cultivated and employed in an *in vitro* cytotoxicity test according to earlier research.[23] The cells were taken from the cell bank of the Chinese Academy of Sciences in Shanghai. Briefly, RAW264.7 cells were inoculated to 96-well plates (5×10^3 cells/well). Twenty-four hours later, the cells either received or not received various dosages of samples at 6.25, 12.5, 25, 50, and 100 μM, respectively, for another 24 h. Then, 10 μL of MTT working solution (dissolved in PBS to 5 mg/mL) and 90 μL of Dulbecco's Modified Eagle Media were added to all well to an additional 4 h. After the addition of 150 μL of DMSO solution, the absorbency of the tested samples were measured at 570 nm. Cell viability was computed through eq 4

$$\text{cell viability (\%)} = [\text{OD}_S/\text{OD}_B] \times 100\% \qquad (4)$$

where OD$_S$ and OD$_B$ are the OD values of the cells that received or did not receive different concentrations of different samples. An electron microscope (DM2500, Leica, Wetzlar, Germany) was used to observe cells 4 h after the addition of MTT.

2.14. Anti-Inflammatory Activity. The content of NO in RAW264.7 cells was determined based on the published reports.[6] Briefly, the RAW264.7 cells (2×10^5 cells/well) were
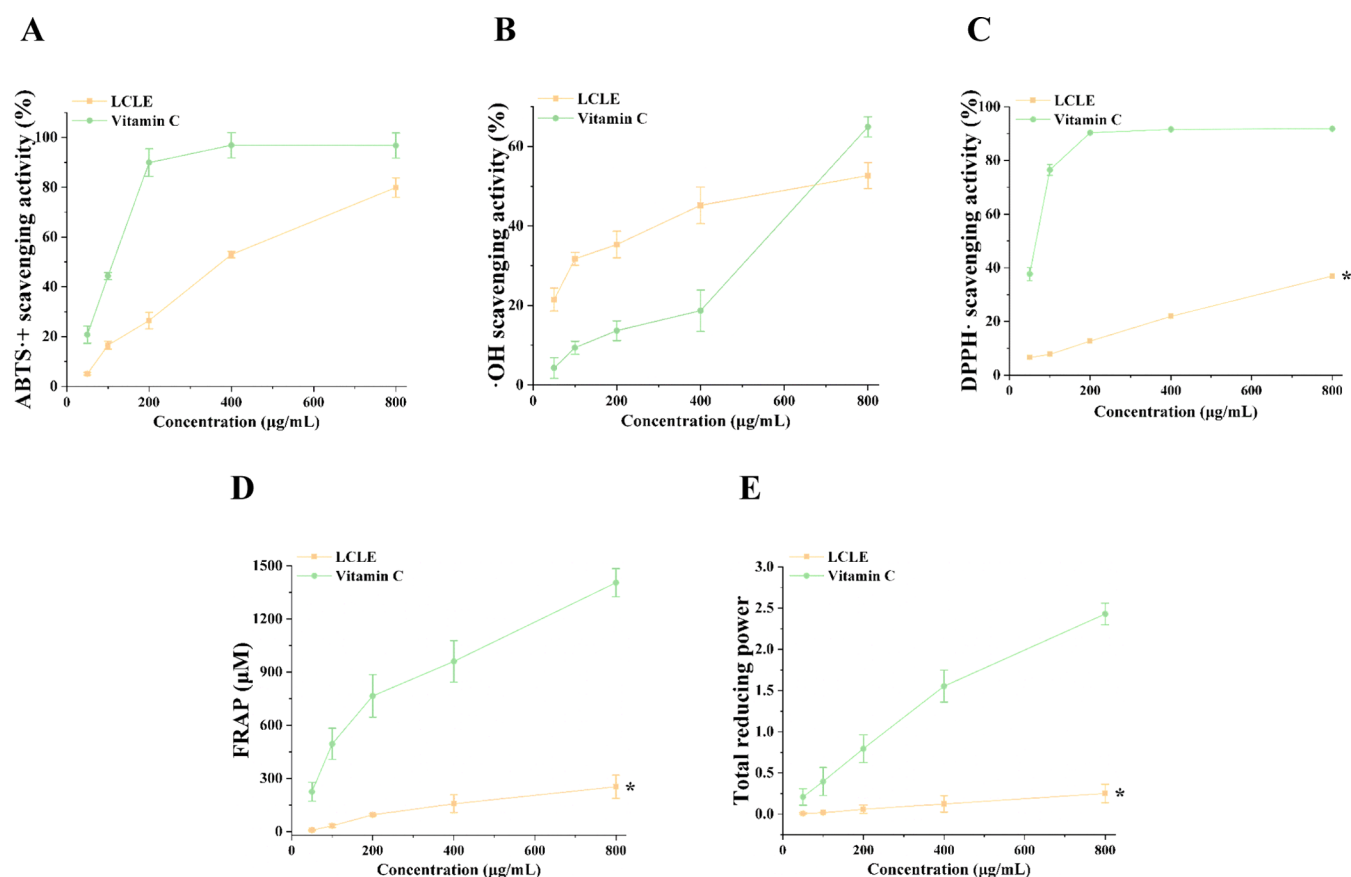
Figure 2. Antioxidant activity of LCLE: (A) ABTS$^{\bullet+}$ scavenging activities; (B) $^{\bullet}$OH scavenging activities; (C) DPPH$^{\bullet}$ scavenging activities; (D) FRAP value; and (E) total reducing power. At least three replications of each experiment were conducted. The data was reported as mean $\pm$ SD.

put onto 24-well plates and exposed or not exposed to different concentrations of test samples for 1 day. Then, the supernatants of cells were used to measure the NO contents.

2.15. RT-qPCR Assay. RT-qPCR assay was accessed according to the published method with modifications.[15] In brief, 1 mL of TRIzol reagent was used to extract the total RNA of RAW264.7 cells. Then, the concentration was determined and the total RNA was purified by employing a NanoDrop 2000C spectrophotometer. Three micrograms of total RNA was used to reverse-transcribe the cDNA by the Transcriptor First Strand cDNA Synthesis Kit. Next, we used the FastStar DNA Master SYBR Green I kit (Roche, Basel, Switzerland) to amplify 75 ng of cDNA by RT-qPCR based on manufacturers' instructions. Finally, the content of the target-expressed genes was computed according to the $2^{-\Delta\Delta CT}$ method.

2.16. Statistical Analysis. The mean $\pm$ standard deviation (SD) was used to show all of the experimental data from at least three different studies. The comparison of means was done by one-way analysis of variance tests using the SPSS 25.0 software (IBM Corporation, Armonk, New York). $p < 0.05$ was considered statistically significant. #p was used when compared with the CON group, and *p was used when compared with the LPS group.

3. RESULTS

3.1. Antioxidant Activity of LCLE. As shown in Figure 2A, treatment with LCLE at 50−800 μg/mL demonstrated notable scavenging activity against ABTS$^{\bullet+}$ depending on the dosage. The scavenging rate of ABTS positive radicals by

LCLE treatment at a concentration of 800 μg/mL reached a maximum of 80%, close to that of the positive control vitamin C at the same concentration. Figure 2B evidences that LCLE treatment significantly and dose-dependently scavenged $^{\bullet}$OH. Of note, the efficacy of LCLE on scavenging $^{\bullet}$OH was greater than that of vitamin C at the same concentrations when the concentrations were lower than 400 μg/mL. The IC$_{50}$ values of LCLE on scavenging ABTS$^{\bullet+}$ and $^{\bullet}$OH were 344.71 and 618.60 μg/mL, respectively. LCLE administration also displayed scavenging effects against DPPH$^{\bullet}$, although the potency was lower than that of vitamin C (Figure 2C). Specifically, the DPPH$^{\bullet}$ scavenging rate by LCLE intervention at 800 μg/mL was close to 40%. In addition, LCLE addition showed a minor reducing power, as evidenced by the FRAP values (Figure 2D) and total reducing power (Figure 2E). These data showed that LCLE had significant antioxidant potential.

3.2. Antibacterial Activities of LCLE. The antimicrobial activity of LCLE is presented in Table 1. Generally, LCLE showed broad-spectrum antibacterial activity, and Gram-positive bacteria appeared to be more responsive than Gram-negative bacteria. LCLE presented the strongest antimicrobial activity against *S. epidermidis* with an MIC of 4.16 mg/mL. As depicted in Figure 3A, LCLE treatment at 2−8 mg potently inhibited *S. epidermidis*, and the inhibition zone increased dose-dependently to 16.92 mm at a dosage of 8 mg. These data indicated that LCLE most likely exhibited the strongest capacity for inhibition against *S. epidermidis* compared with other tested strains. Thus, SEM analysis was used to further assess the morphological changes of *S. epidermidis* after being

Table 1. Minimum Inhibitory Concentrations and Minimum Bactericidal Concentrations (mg/mL) of LCLE and Chloramphenicol[a]

	MIC (mg/mL)	MBC (mg/mL)
microbial strains	LCLE/chloramphenicol	LCLE/chloramphenicol
S. aureus	6.25/0.015	25.00/0.031
S. epidermidis	4.16/0.062	25.00/0.125
P. aeruginosa	12.50/	25.00/
E. coli	25.00/0.015	33.30/0.031

[a]No inhibition.

handed with LCLE (Figure 3B). As illustrated in Figure 3B(a), normal *S. epidermidis* cells were spherical, well-ranged, and consistent in size and displayed typical grapevine shapes and kept their typical round-surfaced cell membranes. On the contrary, *S. epidermidis* cells exposed to an MIC concentration of LCLE displayed irregular shapes and different sizes. Moreover, some of the cells presented destroyed bacterial walls and membranes (Figure 3B(b)). Figure 3B(c) shows that round structures were lost and some of the cell membranes were entirely damaged in *S. epidermidis* cells treated with LCLE at 2 × MIC concentration. In the meantime, the bacteria broke down, the internal stuff leaked out, and the quantity of cells drastically dropped. Obviously, substantial cell membrane damage in *S. epidermidis* cells suggested that LCLE likely exhibited antibacterial activity by changing the structure of *S. epidermidis*.

3.3. Effects of LCLE on Macro Indicators in Mice with ALI Caused by LPS.
As shown in Figure 4A, the body weights of mice in the LCLE-treated groups were slightly higher than those in the CON and LPS groups, indicating the good health condition of mice in each group. The liver index (Figure 4B) and lung index (Figure 4C) were noticeably higher after being induced by LPS, but were significantly reduced to the CON group level after being treated with LCLE. The increase in organ index reflects the severity of its inflammatory evidence. These results supported LCLE's beneficial effects on liver and lung inflammation and stimulated further investigation of the LCLE's anti-inflammatory effects on these organs. The lung

wet/dry ratio was also evaluated to indicate pulmonary edema. As shown in Figure 4D, after treatment with LPS, the lung wet/dry ratios were significantly higher than those in the CON group. However, treatment with LCLE efficiently recovered the lung wet/dry ratios to a normal state.

3.4. Impact of LCLE on Histological Alterations in the Lung and Liver Tissues of Mice with ALI Caused by LPS.
The histopathological changes of the lungs and liver in mice with ALI caused by LPS were determined by HE staining. As shown in Figure 4E, the LPS group exhibited significant damages of lung tissues, as characterized by hemorrhage, thicker alveolar wall, and inflammatory cells infiltrated into the interstitium and alveolar space. In contrast, treatment with LCLE at 100 and 200 mg/kg·day significantly alleviated these alterations. Figure 4F depicts that the liver in the CON group presented a normal structure, central vein, and clearly visible surrounding hepatic cord. In the LPS group, the hepatocytes around the central vein developed focal necrosis, neutrophil infiltration, and congestion of the hepatic sinusoids. However, these conditions were significantly relieved after LCLE treatment. Briefly, the liver tissues in the LPS + H-LCLE group exhibited normal structures similar to those in the CON group, whereas the LPS + L-LCLE group's hepatic sinusoids displayed some mild congestion but otherwise had normal cord-like structures.

3.5. LCLE Inhibited NO and Cytokine Production in LPS-Induced ALI Mice.
As illustrated in Figure 4, NO (Figure 5A), TNF-α (Figure 5B), and IL-6 (Figure 5C) levels were significantly elevated in mice with ALI caused by LPS compared with the CON group. Nevertheless, LCLE administration significantly attenuated this condition. Particularly, TNF-α concentrations in the lung of the LPS + L-LCLE and LPS + H-LCLE groups were markedly decreased to 307.11 ± 10.68 and 368.89 ± 115.65 pg/mL, respectively, close to that in the CON group (Figure 5B).

3.6. Isolation, Purification, and Structural Elucidation of Compounds.
The chemical structures of these three compounds were confirmed by the NMR spectroscopy and HPLC results as below.
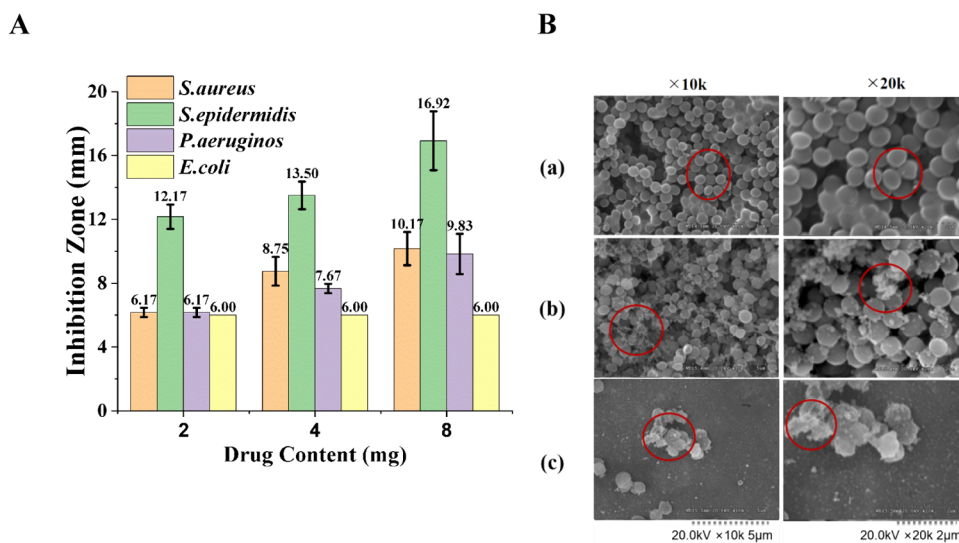
A

B

Figure 3. Bactericidal activities of LCLE: (A) inhibition zone; (B) SEM images of *S. epidermidis*, (a) not received, (b) received LCLE at 1 × MIC, and (c) received LCLE at 2 × MIC. At least three replications of each experiment were conducted. The data was reported as mean ± SD.
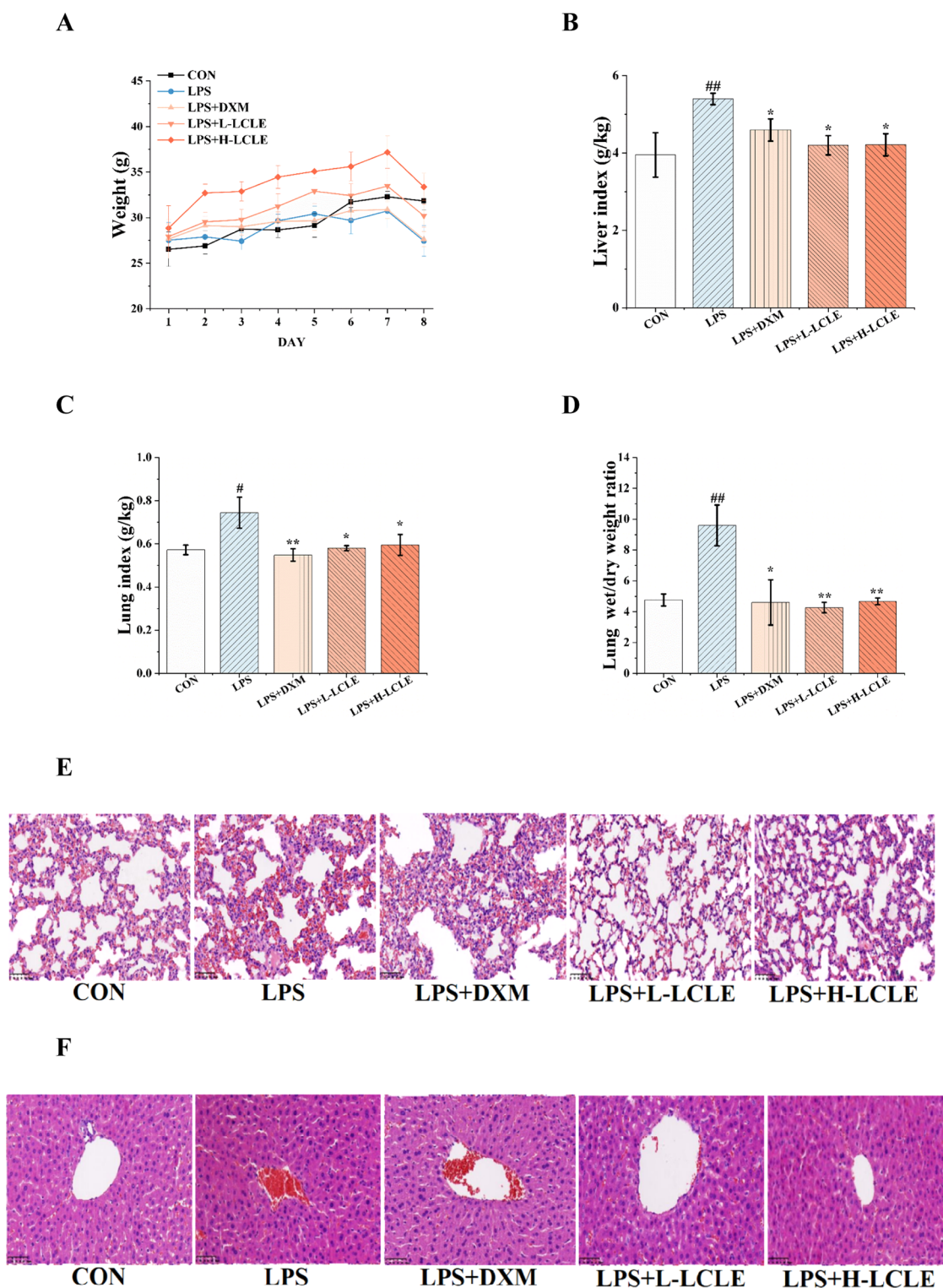
Figure 4. Macro effects and histopathological characteristics of LCLE in mice with ALI caused by LPS: (A) weight; (B) liver index; (C) lung index; (D) left lung wet/dry; (E) representative HE-stained lung sections; and (F) liver sections (50 μm). At least three replications of each experiment were conducted. The data was reported as mean $\pm$ SD.

3.6.1. Fragransin B2. As shown in Table 2, white needle crystal, ^{1}H NMR (600 MHz, The CDCl$_3$) spectrum showed three methoxy hydrogen signals: δ 3.90 (6H, s, 3′-OCH$_3$, 5′-OCH$_3$), 3.88 (3H, m, 3″-OCH$_3$), 3.85 (3H, M, 5″-OCH$_3$); 2 methyl hydrogen signals: δ 1.06 (3H, d, J = 5.85 Hz, 3-CH$_3$), 1.06 (3H, d, J = 5.91 Hz, 4-CH$_3$); 2 aromatic hydrogen signals: δ 6.64 (2H, s, H-2′, H-6′), 6.51(2H, s, H-2″, 6″); 2 secondary

methyl signals: δ 4.62 (2H, d, J = 8.84 Hz, H-2, 5), 1.78 (2H, m, H-3, 4).

The ^{13}C NMR spectrum and the DEPT-135 (150 MHz, CDCl$_3$) spectrum showed a total of 14 carbon signals, including 4 methoxylates carbon signals, respectively: δ 56.4 (3″-OCH$_3$), 56.3 (5″-OCH$_3$), 56.2 (3′-OCH$_3$), 51.01 (5′-OCH$_3$); 7 aromatic carbon signals: δ 147.0 (C-3′, C-5′, C-3″,
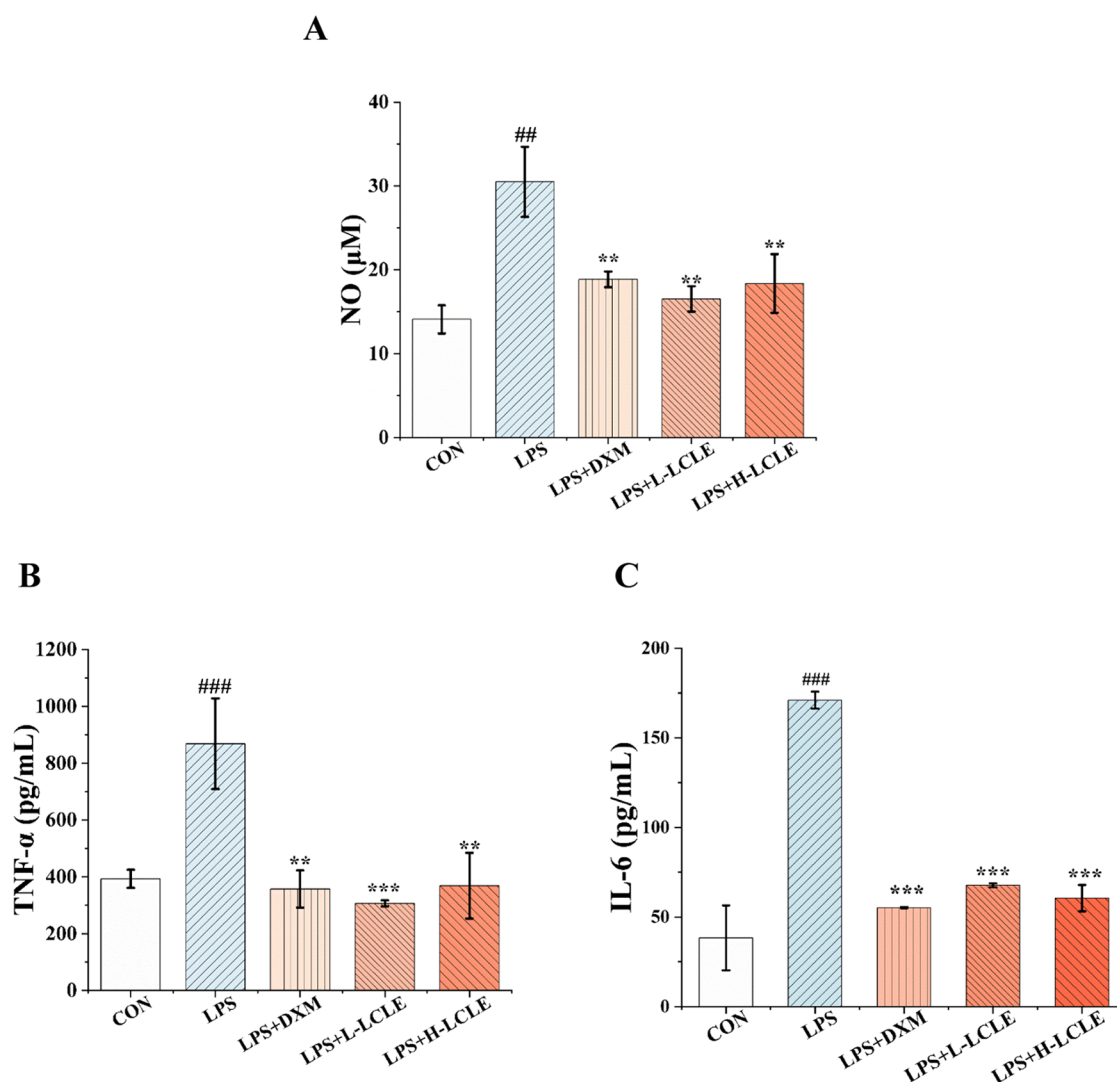
A

B

C

Figure 5. Effects of LCLE on NO and cytokine production in the lung of mice with ALI caused by LPS. (A) NO content; (B) TNF-α content; and (C) IL-6 content. At least three replications of each experiment were conducted. The data was reported as mean ± SD.

C-5″), 134.2 (C-4′, 4″), 133.4 (C-1′, 1″), 103.8 (C-6′), 103.3 (C-2′), 102.9 (C-6″), 102.2 (C-2″); 1 methyl carbon signal: δ 13.9 (3-CH$_3$, 4-CH$_3$); 2 secondary methyl carbon signals: δ 88.7 (C-2, 5), 51.1 (C-3, 4).

Combined with the above data and related references, the structure of compound 1 was identified as fragransin B2 (Figure 6A).[24] And the HPLC retention time for fragransin B2 was 34.487 min (Figure S1A).

3.6.2. Liriodendritol. As depicted in Table 3, white crystal, ^{1}H NMR (600 MHz, D$_2$O) spectrum showed: δ3.08 (1H, dd, J = 5.08 Hz, 4.72 Hz, H-5), 3.28 (2H, m, H-1, 4), 3.33 (3H, H, H-7), 3.47 (1H, H, H-6), 3.49 (3H, m, H-8), 3.56 (1H, m, H-2), 4.19 (1H, m, H-3).

The ^{13}C NMR spectrum and the DEPT-135 (150 MHz, D$_2$O) spectrum showed 8 saturated carbon signals, including 2 methoxylates carbon signals, respectively: δ 56.9 (C-7), 56.7 (C-8); 6 submethyl carbon signals δ 82.3 (C-1), 80.3 (C-4), 73.7 (C-6), 71.6 (C-5), 70.4 (C-2), 67.6 (C-3).

The structure of compound 2 was identified as liriodendritol (Figure 6B).[25] And the HPLC retention time for liriodendritol was 9.857 min (Figure S1B).

3.6.3. Rhamnocitrin. As shown in Table 4, yellow powder, ^{1}H-hydrogen signal (3H, H, 3−11); 4 aromatic hydrogen signals: δ 8.11 (2H, d, J = 8.84 Hz, H-2′, 6′), 6.90 (2H, d, J = 7.95 Hz, H-3′, 5′), 6.60 (1H, s, H-8), 6.30 (1H, s, H-6).

The ^{13}C NMR spectrum and the DEPT-135 (150 MHz) spectrum showed 13 carbon signals, including 1: δ 54.9 (C-11); 9 aromatic carbon signals: δ 166.0 (C-7), 161.5 (C-9), 159.2(C-5), 129.4 (C-2′, 6′), 122.4 (C-1′), 114.9 (C-3′, 5′), 104.2 (C-10), 97.2 (C-6), 91.3 (C-8); 1 base carbon signal: δ 176.2 (C-4); 2 alkene carbon signals: δ 146.6 (C-2), 136.0 (C-3).

Combining the above data and related references, compound 3′s structure was determined to be rhamnocitrin (Figure 6C).[26] And the HPLC retention time for rhamnocitrin was 30.660 min (Figure S1C).

The HPLC analysis confirmed the presence of three compounds in LCLE. The three highest peaks in the HPLC chromatogram of LCLE matched these compounds, and their intensity levels aligned with the mass trend of the isolated compounds (Figure S1D).

3.7. Fragransin B2, Liriodendritol, and Rhamnocitrin Inhibited NO Production in RAW264.7 Cells Caused by

Table 2. ^{1}H NMR (600 MHz) and ^{13}C NMR (150 MHz) Spectral Data of Fragransin B2 (δ in ppm) in CDCl$_3$

position	δ^1H (mult, J in Hz)	δ^{13}C
2	4.62 (d, 8.84)	88.7
3	1.78 (m)	51.1
4	1.78 (m)	51.1
5	4.62 (d, 8.84)	88.7
6	1.06 (d, 5.85)	13.9
7	1.06 (d, 5.91)	13.9
1′		133.4
2′	6.64 (s)	103.3
3′		147.0
4′		134.2
5′		147.0
6′	6.64 (s)	103.8
7′	3.90 (s)	56.2
8′	3.90 (s)	51.0
1″		133.4
2″	6.51 (s)	102.2
3″		147.0
4″		134.2
5″		56.4
6″	6.51 (s)	102.9
7″	3.88 (m)	147.0
8″	3.85 (m)	56.3

Table 3. ^{1}H NMR (600 MHz) and ^{13}C NMR (150 MHz) Spectral Data of Liriodendritol (δ in ppm) in D$_2$O

position	δ^1H (mult, J in Hz)	δ^{13}C
1	3.28 (m)	82.3
2	3.56 (m)	70.4
3	4.19 (m)	67.6
4	3.28 (m)	51.1
5	3.08 (dd, 5.08, 4.72)	71.6
6	3.47 (br s)	73.7
7	3.33 (br s)	56.9
8	3.49 (br s)	56.7

Table 4. ^{1}H NMR (600 MHz) and ^{13}C NMR (150 MHz) Spectral Data of Rhamoncitrin (δ in ppm) in CD$_3$OD

position	δ^1H (mult, J in Hz)	δ^{13}C
2		146.6
3		136.0
4		176.2
5		159.2
6	6.30	97.2
7		166.0
8	6.60 (s)	91.3
9		161.5
10		104.2
11	3.88 (s)	54.9
1′		122.4
2′	8.11 (d, 8.84)	129.4
3′	6.90 (d, 8.84)	114.9
4′		147.0
5′	6.90 (d, 8.84)	114.9
6′	8.11 (d, 8.84)	129.4

LPS. Following treatment with fragransin B2, liriodendritol, and rhamnocitrin, the vitality of RAW264.7 cells surpassed 80%, as demonstrated in Figure 7A. Meanwhile, RAW264.7 cells retained normal shape and size and exhibited intact structures after administration of these three compounds (Figure 7B). These data indicated that these three compounds did not show evident cytotoxicity on RAW264.7 cells. Figure 7C shows that LPS induced RAW264.7 cells to produce substantial intracellular NO. However, NO accumulation in RAW264.7 cells was significantly and dose-dependently reduced when treated with fragransin B2, liriodendritol, and rhamnocitrin at various concentrations. Specifically, rhamnocitrin treatment at 100 μM exhibited the highest inhibition ratio on NO production. Consistently, the morphological changes of RAW264.7 cells by fragransin B2, liriodendritol, and rhamnocitrin intervention also confirmed this (Figure 7D).

3.8. Fragransin B2, Liriodendritol, and Rhamnocitrin Regulated IL-10, IL-1β, IL-6, TNF-α, COX-2, and iNOS mRNA Expression in RAW264.7 Cells Caused by LPS. As shown in Figure 8A, the IL-10 mRNA expression level in the LPS group was significantly lower than that of the CON group. However, treatment of fragransin B2, liriodendritol, and rhamnocitrin markedly inhibited this decrease. LPS induced elevations in pro-inflammatory gene expression levels. These genes including IL-1β (Figure 8B), IL-6 (Figure 8C), TNF-α (Figure 8D), COX-2 (Figure 8E), and iNOS (Figure 8F) were also remarkably reduced by fragransin B2, liriodendritol, and rhamnocitrin administration. As expected, these three compounds exhibited differential inhibition on the expression levels of these genes. Specifically, fragransin B2 was more effective in inhibiting TNF-α mRNA expression, while IL-6 mRNA expression was more effectively inhibited by rhamnocitrin.

4. DISCUSSION

L. tulipifera L. has been shown in numerous research studies to possess antibacterial, anti-inflammatory, and antioxidant effects. For example, the ethanol extract of *L. tulipifera* L. leaves potently inhibited TNF-α-induced inflammatory reactions in RAW264.7 cells.[12,27,28] However, limited attention was focused on *L. chinense*. Herein, we sought to explore whether *L. chinense* possessed comparable pharmacological properties. In
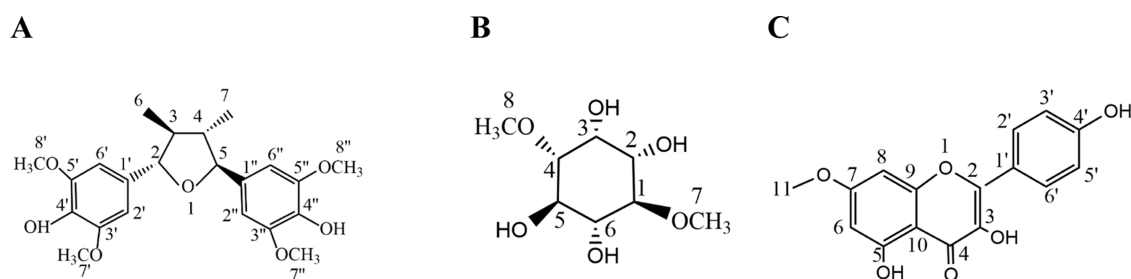

Figure 6. Chemical structures of compounds isolated and identified from LCLE: (A) fragransin B2; (B) liriodendritol; and (C) rhamnocitrin.
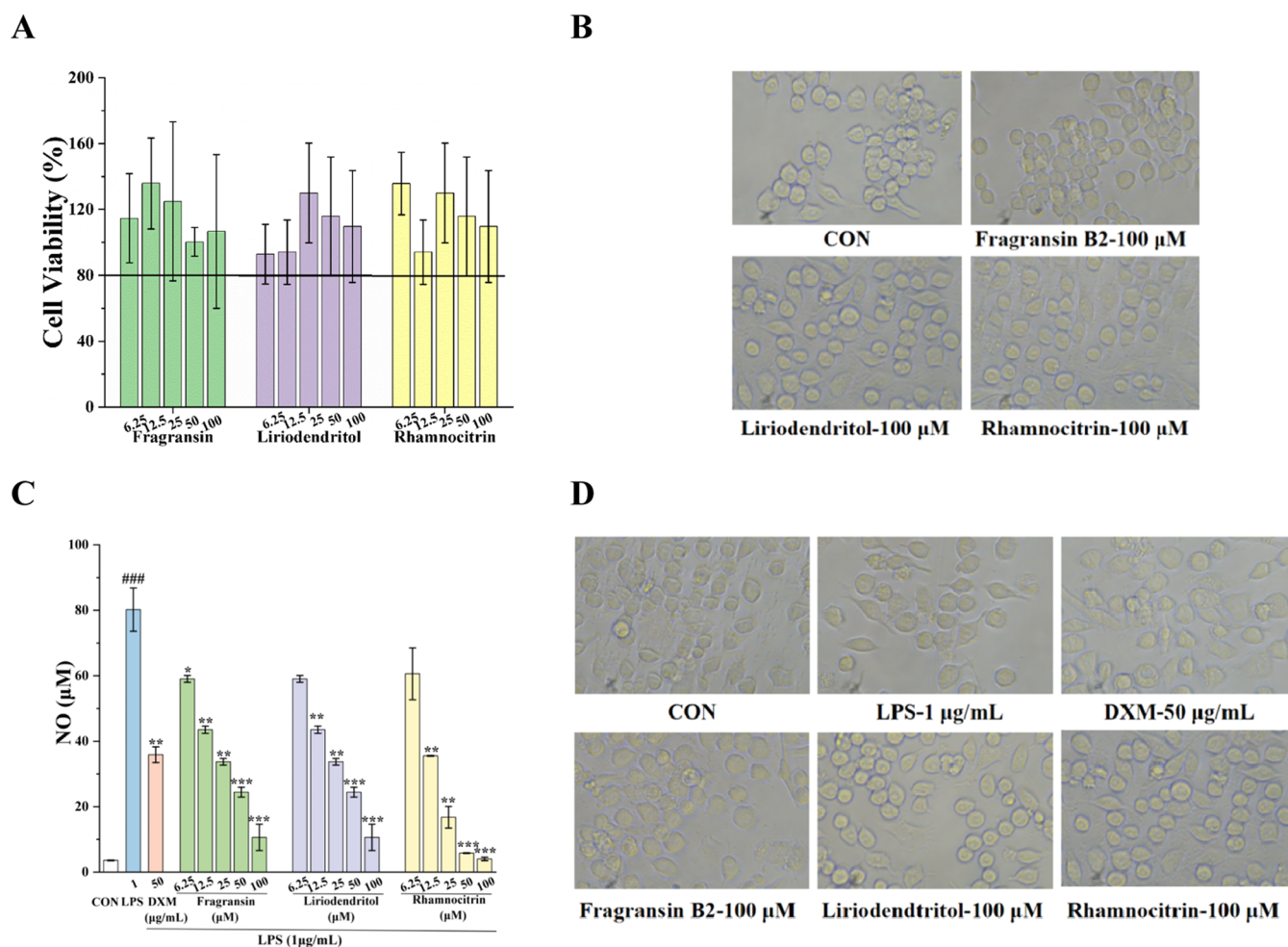
Figure 7. Effects of fragransin B2, liriodendritol, and rhamnocitrin on NO production in RAW264.7 cells caused by LPS. (A) Cytotoxicity; (B) morphological changes; (C) NO content; and (D) morphological changes. At least three replications of each experiment were conducted. The data was reported as mean ± SD.

the current study, LCLE was extracted and isolated from *L. chinense*, and then *in vitro* antioxidant and antibacterial properties as well as *in vivo* effects on LPS-induced ALI in mice of LCLE were investigated. More importantly, three compounds were isolated and identified from LCLE. Furthermore, the effects of these three compounds on inflammatory responses in RAW264.7 cells caused by LPS were comparatively measured to explore the potential compounds responsible for the observed bioactivities of *L. chinense* leaves.

ALI is characterized by swift and intense inflammatory responses from the activation of oxidizing and inflammatory mediator pathways, which cause lung tissue damage to the alveolar epithelium, interstitial edema, and neutrophil build-up.[29,30] In the present study, organ indexes and histopathological features in the lung and liver of the LPS group displayed significant alterations compared with the CON group. These observations implied the successful induction of ALI in mice. The lung wet/dry weight ratio, generally considered as a direct and critical indicator of ALI, also illustrated the amelioration of LPS-induced pulmonary edema by LCLE treatment. Consequently, it was inferred that LCLE could potentially attenuate inflammatory responses in the LPS-mediated ALI in mice. As expected, further assays demonstrated that LCLE intervention significantly inhibited NO and cytokine produc-

tion in LPS-induced ALI mice. Notably, a lower dose of LCLE shows more effect in decreasing NO and TNF-α content. The intricate composition of LCLE, encompassing a variety of compounds with both antagonistic and synergistic properties, likely contributes to this phenomenon. Specific constituents demonstrate differing effects on the synthesis of cellular inflammatory factors dependent on their concentration. While some compounds stabilize the reduction of cellular inflammatory factors at particular concentrations, others exacerbate their increase. As a result, the overall influence of anti-inflammatory cytokines is attenuated.

ALI has a high mortality rate and involves complicated pathogenesis. Inflammatory cells proliferate and become activated in the lung in response to various factors, as well as also emit pro-inflammatory substances such as reactive oxygen species, TNF-α, interleukins, and elastase, thereby promoting the inflammatory cascades. Oxidative stress represents a significant cause of the damage of pulmonary vascular endothelial cells and the dysfunction of alveolar epithelial cells. The balance between oxidation and antioxidants is crucial for vascular homeostasis, and antioxidants have progressively become a pivotal approach for the treatment of ALI.[28] In this context, we investigated whether LCLE acted by inhibiting oxidative stress. As expected, LCLE demonstrated remarkable scavenging effects against ABTS$^{\bullet+}$, $^{\bullet}$OH, and DPPH$^{\bullet}$. Of
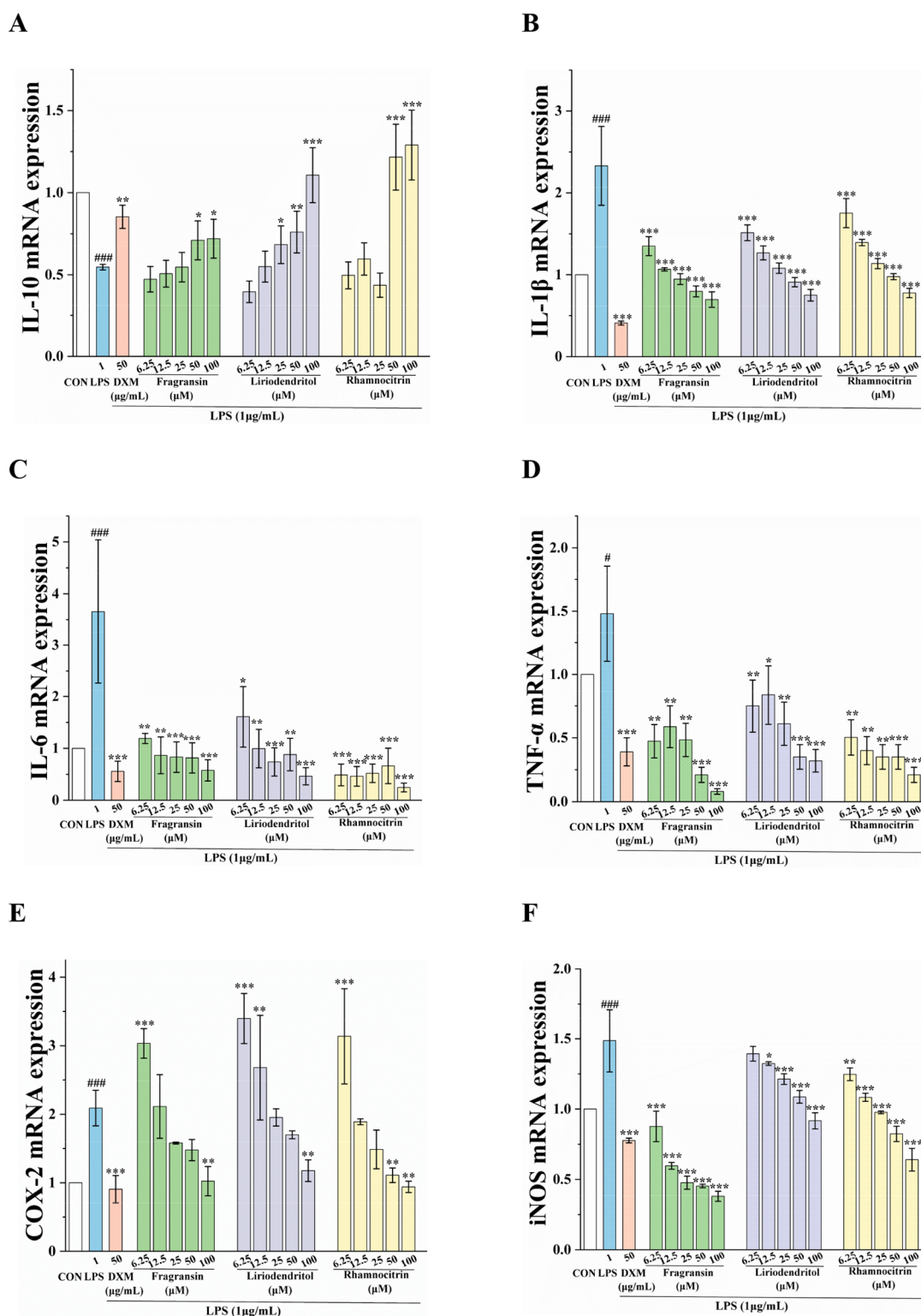
Figure 8. Effects of fragransin B2, liriodendritol, and rhamnocitrin on inflammatory-related gene expression levels in RAW264.7 cells caused by LPS. (A) IL-10; (B) IL-1β; (C) IL-6; (D) TNF-α; (E) COX-2; and (F) iNOS. At least three replications of each experiment were conducted. The data was reported as mean ± SD.

particular note was LCLE's superior efficacy on scavenging ABTS$^{\bullet+}$ and $^{\bullet}$OH radicals, with IC$_{50}$ values of 344.71 and 618.60 μg/mL, respectively. In support, essential oil from *L. tulipifera* L. leaves also exhibited significant scavenging capacities on DPPH$^{\bullet}$ and ABTS$^{\bullet+}$.[28]

E. coli, P. aeruginosa, S. aureus, and *S. epidermidis* are frequently encountered germs in the lung, particularly detrimental to lung health and potentially leading to ALI.[31,32] Thus, our research used MIC, MBC, and disc diffusion assays to determine the antibacterial activity of LCLE

against four strains of bacteria, both Gram-positive and Gram-negative. The results showed that LCLE possessed a broad-spectrum antibacterial effect. The inhibitory components of LCLE might enter the bacterium to impede the production of free radicals such as ABTS[•+] and [•]OH radicals.[33] To uncover how LCLE functions with its antibacterial ability, we determined the morphological alterations of the germs by SEM. SEM examination of *S. epidermidis* indicated that the mechanism of LCLE might entail the dose-dependent disruption of bacterial structures. Nevertheless, a comprehensive elucidation of the antibacterial mechanism of LCLE necessitates additional experiments, for instance, measuring the leaking of nucleic acids and alkaline phosphatase activity into the bacterial to detect the integrity of cell wall and using transmission electron microscopy to observe how LCLE interacts with and affects bacterial membranes and cytoplasm.[34,35]

To identify the potential compounds responsible for the observed bioactivity of LCLE, three compounds including fragransin B2, liriodendritol, and rhamnocitrin were isolated and purified from LCLE. Although these three compounds are not novel, fragransin B2 and rhamnocitrin were newly discovered constituents in LCLE. The primary cause and presentation of ALI is the inflammatory response. Therefore, our research delves into identifying the possible anti-inflammatory components of LCLE that ameliorate ALI. Subsequently, further comparative research using RAW264.7 cells caused by LPS was done to investigate and validate these three compounds' ability to reduce inflammation *in vitro*. As expected, fragransin B2, liriodendritol, and rhamnocitrin presented differential regulation on NO production and IL-10, IL-1β, IL-6, TNF-α, COX-2, and iNOS mRNA expression levels in RAW264.7 cells caused by LPS, with rhamnocitrin the most effective. In line with previous research, rhamnocitrin exhibits anti-inflammatory properties, potentially acting as the key active constituent of LCLE.[36] Rhamnocitrin with superior anti-inflammatory activity was probably owing to its flavonoid nature, with the 5-hydroxy structure of flavonoids playing a decisive role in NO production.[37]

Upon LPS stimulation, RAW264.7 cells swiftly emulate the inflammatory microenvironment, resulting in the rapid production and release of many inflammatory substances and receptors.[38] TNF-α, IL-1β, IL-6, IL-10, and NO are examples of inflammatory mediators that are essential to inflammation. IL-6, a versatile and dynamic molecule, functions as an intermediary mediator of inflammation with diverse roles.[6] As a notable early inflammation marker, IL-6 is released by macrophages, and TNF-α and IL-1β stimulate its production and secretion. The majority of immune cells also induce COX-2 expression during the period of inflammation.[39] Our findings suggested that fragransin B2, liriodendritol, and rhamnocitrin probably exhibited inflammatory-fighting effects by preventing the expression of iNOS, TNF-α, IL-1β, IL-6, and COX-2 mRNA, thereby decreasing the levels of NO, TNF-α, and IL-1β, while simultaneously elevating IL-10 mRNA expression. Interestingly, it was noted that fragransin B2 exhibited strong inhibition on iNOS, IL-1β, and especially TNF-α mRNA expression but a weak promotion on IL-10 mRNA expression. Rhamnocitrin was more powerful in inhibiting IL-6 and COX-2 mRNA expression and increasing IL-10 mRNA expression. However, gaining a comprehensive understanding of the anti-inflammatory mechanism of fragransin B2, liriodendritol, and rhamnocitrin necessitates further in-depth experiments, such as

investigations using human cell lines and additional clinical trials.[40−42] These facts evidenced that different compounds probably manifested different biological activities. The observed efficacy of LCLE was probably achieved by the synergistic effects of all of the compounds.

In conclusion, LCLE possessed significant antioxidant and antimicrobial activities along with its potential to mitigate LPS-induced ALI in mice. Also, this study revealed the pivotal roles of fragransin B2 and rhamnocitrin in mitigating LPS-induced inflammation. These investigations contributed to the pharmacological knowledge of *L. chinense* leaves and offered a chance to continue developing better medications for acute lung injuries that have fewer adverse effects. However, because of the enormous workload, only the relevant activity of the liriodendron leaf 60% alcohol extract was examined; the alcohol extract of each gradient was not carried out. It may include gradients protecting against acute lung injury as well.

■ ASSOCIATED CONTENT

ⓈI Supporting Information

The Supporting Information is available free of charge at https://pubs.acs.org/doi/10.1021/acsomega.3c10269.

> HPLC analysis of reference compounds and LCLE; the TCL results of compounds 1 and 3. ^{1}H (600 MHz) NMR spectrum, ^{13}C (150 MHz) NMR spectrum, and DEPT (150 MHz) NMR spectrum of fragransin B2, liriodendritol, and rhamoncitrin, respectively (PDF)

■ AUTHOR INFORMATION

Corresponding Authors

Cui-Ping Jiang − *School of Traditional Chinese Medicine, Southern Medical University, Guangzhou 510515, China; Guangdong Provincial Key Laboratory of Chinese Medicine Pharmaceutics, Southern Medical University, Guangzhou 510515, China; Guangdong Basic Research Center of Excellence for Integrated Traditional and Western Medicine for Qingzhi Diseases, Guangzhou 510515, China;* ⓞ orcid.org/0000-0001-9694-5399; Phone: +86-20-61648263; Email: cuipingjiangcpu@163.com; Fax: +86-20-61648263

Qun Shen − *School of Traditional Chinese Medicine, Southern Medical University, Guangzhou 510515, China; Guangdong Provincial Key Laboratory of Chinese Medicine Pharmaceutics, Southern Medical University, Guangzhou 510515, China; Guangdong Basic Research Center of Excellence for Integrated Traditional and Western Medicine for Qingzhi Diseases, Guangzhou 510515, China;* Phone: +86-20-61648542; Email: 2451221@qq.com; Fax: +86-20-61648542

Chun-Yan Shen − *School of Traditional Chinese Medicine, Southern Medical University, Guangzhou 510515, China; Guangdong Provincial Key Laboratory of Chinese Medicine Pharmaceutics, Southern Medical University, Guangzhou 510515, China; Guangdong Basic Research Center of Excellence for Integrated Traditional and Western Medicine for Qingzhi Diseases, Guangzhou 510515, China;* ⓞ orcid.org/0000-0002-4370-2147; Phone: +86-20-61648263; Email: shenchunyan@smu.edu.cn; Fax: +86-20-61648263

Authors

Ya-Li Wang − *School of Traditional Chinese Medicine, Southern Medical University, Guangzhou 510515, China; Guangdong Provincial Key Laboratory of Chinese Medicine Pharmaceutics, Southern Medical University, Guangzhou 510515, China; Guangdong Basic Research Center of Excellence for Integrated Traditional and Western Medicine for Qingzhi Diseases, Guangzhou 510515, China*

Qian Ni − *School of Traditional Chinese Medicine, Southern Medical University, Guangzhou 510515, China; Guangdong Provincial Key Laboratory of Chinese Medicine Pharmaceutics, Southern Medical University, Guangzhou 510515, China; Guangdong Basic Research Center of Excellence for Integrated Traditional and Western Medicine for Qingzhi Diseases, Guangzhou 510515, China*

Wen-Hao Zeng − *School of Traditional Chinese Medicine, Southern Medical University, Guangzhou 510515, China; Guangdong Provincial Key Laboratory of Chinese Medicine Pharmaceutics, Southern Medical University, Guangzhou 510515, China; Guangdong Basic Research Center of Excellence for Integrated Traditional and Western Medicine for Qingzhi Diseases, Guangzhou 510515, China*

Hui Feng − *School of Traditional Chinese Medicine, Southern Medical University, Guangzhou 510515, China; Guangdong Provincial Key Laboratory of Chinese Medicine Pharmaceutics, Southern Medical University, Guangzhou 510515, China; Guangdong Basic Research Center of Excellence for Integrated Traditional and Western Medicine for Qingzhi Diseases, Guangzhou 510515, China*

Wei-Feng Cai − *School of Traditional Chinese Medicine, Southern Medical University, Guangzhou 510515, China; Guangdong Provincial Key Laboratory of Chinese Medicine Pharmaceutics, Southern Medical University, Guangzhou 510515, China; Guangdong Basic Research Center of Excellence for Integrated Traditional and Western Medicine for Qingzhi Diseases, Guangzhou 510515, China*

Qi-Cong Chen − *School of Traditional Chinese Medicine, Southern Medical University, Guangzhou 510515, China; Guangdong Provincial Key Laboratory of Chinese Medicine Pharmaceutics, Southern Medical University, Guangzhou 510515, China; Guangdong Basic Research Center of Excellence for Integrated Traditional and Western Medicine for Qingzhi Diseases, Guangzhou 510515, China*

Song-Xia Lin − *School of Traditional Chinese Medicine, Southern Medical University, Guangzhou 510515, China; Guangdong Provincial Key Laboratory of Chinese Medicine Pharmaceutics, Southern Medical University, Guangzhou 510515, China; Guangdong Basic Research Center of Excellence for Integrated Traditional and Western Medicine for Qingzhi Diseases, Guangzhou 510515, China*

Yan-Kui Yi − *School of Traditional Chinese Medicine, Southern Medical University, Guangzhou 510515, China; Guangdong Provincial Key Laboratory of Chinese Medicine Pharmaceutics, Southern Medical University, Guangzhou 510515, China; Guangdong Basic Research Center of Excellence for Integrated Traditional and Western Medicine for Qingzhi Diseases, Guangzhou 510515, China*

Complete contact information is available at:
https://pubs.acs.org/10.1021/acsomega.3c10269

Author Contributions

‖Y.-L.W. and Q.N. contributed equally to this work. Y.-L.W.: Writing, methodology, conceptualization. Q.N.: Writing, methodology, investigation. W.-H.Z.: Validation. H.F.: Data curation. W.-F.C.: Methodology, investigation. Q.-C.C.: Methodology, investigation. S.-X.L.: Methodology. C.-P.J.: Investigation. Y.-K.Y.: Investigation. Q.S.: Conceptualization, review, supervision. C.-Y.S.: Review, supervision, project administration. All authors have read and approved the manuscript.

Notes

Ethical approval was granted by the ethical committee, the Animal Ethics Committee established by Southern Medical University (Guangzhou, China, L2021084). All animals used in the experiment were handled and treated by ethical standards that had been authorized by an ethical committee. The authors declare no competing financial interest.

ABBREVIATIONS

ABTS, 2,2′-biazo-bis-3-ethyl-benzothiazoline-6-sulfonic acid; ALI, acute lung injury; CON, control group; COX-2, cyclooxygenase-2; D, dry weight; DPPH, 1,1-diphenyl-2-picrylhydrazyl; DXM, dexamethasone group; *E. coli, Escherichia coli*; ELISA, enzyme-linked immunosorbent assay; FRAP, ferric reducing antioxidant power; GDMCC, Guangdong Microbial Culture Collection Center; HE, hematoxylin and eosin; IL-6, interleukin-6; iNOS, nitric oxide synthase; LCLE, ethanol extract of *L. chinense*; LPS, lipopolysaccharide; LPS + H-LCLE, high-dose LCLE group; LPS + L-LCLE, low-dose LCLE group; MBC, minimum bactericidal concentrations; MIC, minimum inhibitory concentrations; MTT, 3-(4,5-dimethyl-2-thiazolyl)-2,5-diphenyl-2*H*-tetrazolium bromide; NO, nitric oxide; *P. aeruginosa, Pseudomonas aeruginosa*; *S. aureus, Staphylococcus aureus*; SEM, scanning electron microscope; *S. epidermidis, Staphylococcus epidermidis*; TNF-α, tumor necrosis factor-α; W, wet weight

REFERENCES

(1) Ahmad, A. A.; Hussain, K.; Shah, M. R.; Halimi, S. M. A.; Rabbi, F.; Ahmad, Z.; Khan, I.; Rauf, A.; Alshammari, A.; Alharbi, M.; Suleria, H. A. R. Molecular insights into the *in vivo* analgesic and anti-inflammatory activity of indomethacin Analogues. *ACS Omega* **2023**, *8*, 30048−30056.

(2) Nabil-Adam, A.; Ashour, M. L.; Shreadah, M. A. Modulation of MAPK/NF-κB pathway and NLRP3 inflammasome by secondary metabolites from red Algae: A mechanistic study. *ACS Omega* **2023**, *8*, 37971−37990.

(3) Rahmawati, L.; Aziz, N.; Oh, J.; Hong, Y. H.; Woo, B. Y.; Hong, Y. D.; Manilack, P.; Souladeth, P.; Jung, J. H.; Lee, W. S.; et al. Cissus subtetragona Planch. ameliorates inflammatory responses in LPS-induced macrophages, HCl/EtOH-induced gastritis, and LPS-induced lung injury via attenuation of Src and TAK1. *Molecules* **2021**, *26*, No. 6073.

(4) Peng, F.; Yin, H. Y.; Du, B.; Niu, K.; Yang, Y. D.; Wang, S. J. Anti-inflammatory effect of flavonoids from chestnut flowers in lipopolysaccharide-stimulated RAW 264.7 macrophages and acute lung injury in mice. *J. Ethnopharmacol.* **2022**, *290*, No. 115086.

(5) Shen, C. Y.; Jiang, J. G.; Li, M. Q.; Zheng, C. Y.; Zhu, W. Structural characterization and immunomodulatory activity of novel polysaccharides from Citrus aurantium Linn. variant amara Engl. *J. Funct. Foods* **2017**, *35*, 352−362.

(6) Shen, C. Y.; Zhang, W. L.; Jiang, J. G. Immune-enhancing activity of polysaccharides from Hibiscus sabdariffa Linn. via MAPK and NF-kB signaling pathways in RAW264.7 cells. *J. Funct. Foods* **2017**, *34*, 118−129.

(7) Li, Z. H.; Pan, H. T.; Yang, J. H.; Chen, D. J.; Wang, Y.; Zhang, H.; Cheng, Y. Y. Xuanfei Baidu formula alleviates impaired mitochondrial dynamics and activated NLRP3 inflammasome by repressing NF-*κ*B and MAPK pathways in LPS-induced ALI and inflammation models. *Phytomedicine* **2023**, *108*, No. 154545.

(8) Su, M. L.; Yang, B. W.; Xi, M. R.; Qiang, C.; Yin, Z. N. Therapeutic effect of pH-responsive dexamethasone prodrug nano-particles on acute lung injury. *J. Drug Delivery Sci. Technol.* **2021**, *66*, No. 102738, DOI: 10.1016/j.jddst.2021.102738.

(9) Zhou, L. L.; Shen, Y.; Huang, T. T.; Sun, Y. Y.; Alolga, R. N.; Zhang, G.; Ge, Y. Q. The prognostic effect of dexamethasone on patients with glioblastoma: a systematic review and meta-analysis. *Front. Pharmacol.* **2021**, *12*, No. 727707, DOI: 10.3389/fphar.2021.727707.

(10) Chen, J. H.; Hao, Z. D.; Guang, X. M.; Zhao, C. X.; Wang, P. K.; Xue, L. J.; Zhu, Q. H.; Yang, L. F.; Sheng, Y.; Zhou, Y. W.; et al. Liriodendron genome sheds light on angiosperm phylogeny and species−pair differentiation. *Nat. Plants* **2019**, *5*, 18−25.

(11) He, Y. H.; Li, Q. X.; Wu, Y. F.; Jiang, C. X.; Zhou, Q.; Jin, Z. X.; Chen, W. X.; Mao, Y. C.; Hu, J. F.; Xiong, J. Liriogerphines A−D, a class of sesquiterpene−alkaloid hybrids from the rare Chinese Tulip Tree plant. *J. Org. Chem.* **2022**, *87*, 6927−6933.

(12) Jeong, E. J.; Kim, N. H.; Heo, J. D.; Lee, K. Y.; Rho, J. R.; Kim, Y. C.; Sung, S. H. Antifibrotic compounds from Liriodendron tulipifera attenuating HSC-T6 proliferation and TNF-alpha production in RAW264.7 cells. *Biol. Pharm. Bull.* **2015**, *38*, 228−234.

(13) Pan, J.; Zhang, C. L.; Shi, M.; Guo, F.; Liu, J.; Li, L. Z.; Ren, Q.; Tao, S.; Tang, M. H.; Ye, H. Y.; et al. Ethanol extract of Liriodendron chinense (Hemsl.) Sarg barks attenuates hyperuricemic nephropathy by inhibiting renal fibrosis and inflammation in mice. *J. Ethnopharmacol.* **2021**, *264*, No. 113278.

(14) Kang, Y. F.; Liu, C. M.; Kao, C. L.; Chen, C. Y. Antioxidant and anticancer constituents from the leaves of Liriodendron tulipifera. *Molecules* **2014**, *19*, 4234−4245.

(15) Wang, Y. L.; Lin, S. X.; Wang, Y.; Liang, T.; Jiang, T.; Liu, P.; Li, X. Y.; Lang, D. Q.; Liu, Q.; Shen, C. Y. p-Synephrine ameliorates alloxan-induced diabetes mellitus through inhibiting oxidative stress and inflammation via suppressing the NF-kappa B and MAPK pathways. *Food Funct.* **2023**, *14*, 1971−1988.

(16) Lu, Y. F.; Li, D. X.; Zhang, R.; Zhao, L. L.; Qiu, Z.; Du, Y.; Ji, S.; Tang, D. Q. Chemical antioxidant quality markers of Chrysanthemum morifolium using a spectrum-effect approach. *Front. Pharmacol.* **2022**, *13*, No. 809482, DOI: 10.3389/fphar.2022.809482.

(17) Liu, H. M.; Huang, J. G.; Yang, S. F.; Li, J. L.; Zhou, L. J. Chemical composition, algicidal, antimicrobial, and antioxidant activities of the essential oils of Taiwania flousiana Gaussen. *Molecules* **2020**, *25*, No. 967.

(18) Sarikurkcu, C.; Arisoy, K.; Tepe, B.; Cakir, A.; Abali, G.; Mete, E. Studies on the antioxidant activity of essential oil and different solvent extracts of Vitex agnus castus L. fruits from Turkey. *Food Chem. Toxicol.* **2009**, *47*, 2479−2483.

(19) de la Torre, A. A. S. B.; Henderson, T.; Nigam, P. S.; Owusu-Apenten, R. K. A universally calibrated microplate ferric reducing antioxidant power (FRAP) assay for foods and applications to Manuka honey. *Food Chem.* **2015**, *174*, 119−123.

(20) da Silva, M. M. C.; de Araújo Neto, J. B.; dos Santos, A. T. L.; de Morais Oliveira-Tintino, C. D.; de Araújo, A. C. J.; Freitas, P. R.; da Silva, L. E.; Do Amaral, W.; Deschamps, C.; de Azevedo, F. R.; et al. Antibiotic-potentiating activity of the Schinus terebinthifolius

Raddi essential oil against MDR bacterial Strains. *Plants* **2023**, *12*, No. 1587.

(21) Kong, J.; Xie, Y. F.; Guo, Y. H.; Cheng, Y. L.; Qian, H.; Yao, W. R. Biocontrol of postharvest fungal decay of tomatoes with a combination of thymol and salicylic acid screening from 11 natural agents. *LWT–Food Sci. Technol.* **2016**, *72*, 215−222.

(22) Huang, K.; Liu, R.; Zhang, Y.; Guan, X. Characteristics of two cedarwood essential oil emulsions and their antioxidant and antibacterial activities. *Food Chem.* **2021**, *346*, No. 128970.

(23) Ibrahim, B.; Sowemimo, A.; Spies, L.; Koekomoer, T.; van de Venter, M.; Odukoya, O. A. Antiproliferative and apoptosis inducing activity of Markhamia tomentosa leaf extract on HeLa cells. *J. Ethnopharmacol.* **2013**, *149*, 745−749.

(24) Mahmoud, A. B.; Danton, O.; Kaiser, M.; Han, S.; Moreno, A.; Algaffar, S. A.; Khalid, S.; Oh, W. K.; Hamburger, M.; Mäser, P. Lignans, amides, and saponins from Haplophyllum tuberculatum and their antiprotozoal activity. *Molecules* **2020**, *25*, No. 2825.

(25) Yang, N. Y.; Wang, L. Y.; Zhang, Y. W. Immunological activities of components from leaves of Liriodendron chinensis. *Chin. Herb. Med.* **2015**, *7*, 279−282.

(26) Li, X.; Zhang, S. D.; Jin, H. Z.; Dong, F.; Shan, L.; Zhang, W. D. A new flavonol from Oxytropis ochrocephala Bunge. *Nat. Prod. Res.* **2013**, *27*, 554−557.

(27) Huang, X. B.; Hao, N.; Wang, Q.; Li, R. R.; Zhang, G.; Chen, G. Q.; Liu, S. M.; Che, Z. P. Non-food bioactive forest product liriodenine: Sources, chemistry, and bioactivities. *Ind. Crops Prod.* **2022**, *187*, No. 115447.

(28) Quassinti, L.; Maggi, F.; Ortolani, F.; Lupidi, G.; Petrelli, D.; Vitali, L. A.; Miano, A.; Bramucci, M. Exploring new applications of tulip tree (Liriodendron tulipifera L.): leaf essential oil as apoptotic agent for human glioblastoma. *Environ. Sci. Pollut. Res.* **2019**, *26*, 30485−30497.

(29) Li, J. C.; Lu, K. M.; Sun, F. L.; Tan, S. J.; Zhang, X.; Sheng, W.; Hao, W. M.; Liu, M.; Lu, W. H.; Han, W. Panaxydol attenuates ferroptosis against LPS-induced acute lung injury in mice by Keap1-Nrf2/HO-1 pathway. *J. Transl. Med.* **2021**, *19*, No. 96, DOI: 10.1186/s12967-021-02745-1.

(30) Liu, Y.; Zhou, S. J.; Xiang, D.; Ju, L.; Shen, D. X.; Wang, X. H.; Wang, Y. F. Friend or foe? The roles of antioxidants in acute lung injury. *Antioxidants* **2021**, *10*, No. 1956.

(31) Kumar, V. S.; Sadikot, R. T.; Purcell, J. E.; Malik, A. B.; Liu, Y. Pseudomonas aeruginosa induced lung injury model. *J. Visualized Exp.* **2014**, *92*, No. e52044, DOI: 10.3791/52044.

(32) Zhu, Y. J.; Ge, X. L.; Xie, D.; Wang, S. Y.; Chen, F.; Pan, S. M. Clinical Strains of Pseudomonas aeruginosa secrete LasB Elastase to induce hemorrhagic diffuse alveolar damage in mice. *J. Inflammation Res.* **2021**, *14*, 3767−3780.

(33) Rayan, M.; Abu-Farich, B.; Basha, W.; Rayan, A.; Abu-Lafi, S. Correlation between antibacterial activity and free-radical scavenging: *In-vitro* evaluation of polar/non-polar extracts from 25 plants. *Processes* **2020**, *8* (1), No. 117.

(34) Chen, P. T.; Chen, M. Y.; Peng, C.; Yan, J. H.; Shen, X.; Zhang, W. J.; Yuan, Y. M.; Gan, G. X.; Luo, X. J.; Zhu, W. X.; et al. *In vitro* anti-bacterial activity and its preliminary mechanism of action of the non-medicinal parts of Sanguisorba officinalis L. against Helicobacter pylori infection. *J. Ethnopharmacol.* **2024**, *318*, No. 116981.

(35) Liu, T.; Wang, Z. J.; Shi, Y. Z.; Tao, R.; Huang, H.; Zhao, Y. L.; Luo, X. D. Curcusinol from the fruit of Carex baccans with antibacterial activity against multidrug-resistant strains. *J. Ethnopharmacol.* **2024**, *318*, No. 116892.

(36) de Souza Silva, A. P.; de Camargo, A. C.; Lazarini, J. G.; Franchin, M.; de Cassia Orlandi Sardi, J.; Rosalen, P. L.; de Alencar, S. M. Phenolic profile and the antioxidant, anti-inflammatory, and antimicrobial properties of Acai (Euterpe oleracea) Meal: A prospective study. *Foods* **2022**, *12*, No. 86, DOI: 10.3390/foods12010086.

(37) Jiang, W. J.; Daikonya, A.; Ohkawara, M.; Nemoto, T.; Noritake, R.; Takamiya, T.; Kitanaka, S.; Iijima, H. Structure-activity relationship of the inhibitory effects of flavonoids on nitric oxide

production in RAW264.7 cells. *Bioorg. Med. Chem.* **2017**, *25*, 779−788.

(38) Shen, J. H.; Cao, F.; Huang, Z. Y.; Ma, X. H.; Yang, N. A.; Zhang, H. T.; Zhang, Y. H.; Zhang, Z. Q. Chukrasia tabularis limonoid plays anti-inflammatory role by regulating NF-κB signaling pathway in lipopolysaccharide-induced macrophages. *Food Nutr. Res.* **2023**, *67*, No. 9383, DOI: 10.29219/fnr.v67.9383.

(39) Luo, J. F.; Yue, L.; Wu, T. T.; Zhao, C. L.; Ye, J. H.; He, K.; Zou, J. Triterpenoid and coumarin isolated from astilbe grandis with anti-Inflammatory effects through inhibiting the NF-κB Pathway in LPS-induced RAW264.7 Cells. *Molecules* **2023**, *28*, No. 5731.

(40) Hsieh, P. C.; Peng, C. K.; Huang, K. L.; et al. Aqueous extract of descuraniae semen attenuates lipopolysaccharide-induced inflammation and apoptosis by regulating the proteasomal degradation and IRE1a-dependent unfolded protein response in A549 cells. *Front. Immunol.* **2022**, *13*, No. 916102, DOI: 10.3389/fimmu.2022.916102.

(41) Li, J. C.; Lu, K.; Sun, F. L.; Sun, F.; Tan, S. J.; Tan, S.; Zhang, X.; Zhang, X.; Sheng, W.; Sheng, W.; Hao, W. M.; Hao, W.; Liu, M.; Liu, M.; Lv, W. H.; Lv, W.; Han, W. Panaxydol attenuates ferroptosis against LPS-induced acute lung injury in mice by Keap1-Nrf2/HO-1 pathway. *J. Transl. Med.* **2021**, *19*, No. 96, DOI: 10.1186/s12967-021-02745-1.

(42) Li, P. Y.; Gu, L. B.; Wang, L. J.; et al. Long non-coding RNA MALAT1 enhances the protective effect of dexmedetomidine on acute lung injury by sponging miR-135a-5p to downregulate the ratio of X-box binding proteins XBP-1S/XBP-1U. *Bioengineered* **2021**, *12*, 6377−6389.